Process Optimization of High Surface Area Activated Carbon Prepared from *Cucumis Melo* by H₃PO₄ Activation for the Removal of Cationic and Anionic Dyes Using Full Factorial Design

Aziz El Kassimi [1],[*] 🆔 **, Youness Achour** [1]**, Mamoune El Himri** [1]**, My Rachid Laamari** [1]**, Mohammadine El Haddad** [1],[*] 🆔

[1]   Laboratory of Analytical and Molecular Chemistry (LCAM), Poly-disciplinary Faculty of safi, Cadi Ayyad University, BP 4162, 46000 Safi, Morocco

[*]   Correspondence: azizelkassimi2012@gmail.com (A.E.K.); elhaddad71@gmail.com (M.E,H.);

Abstract: In this study, Chemical activation was used to prepare a low-cost activated carbon (AC) from agricultural waste material: Cucumis melo. It was used as a green biosorbent for the removal of cationic and anionic dyes from aqueous solutions (Methylene blue (MB) and Acid orange 7 (AO7)).A full factorial 2^4 experimental design was used to optimize the preparation conditions. The factors and levels included are activation temperature (300 and 500ºC), activation time (1 and 3 h), H₃PO₄ concentration (1.5 and 2.5 mol/L), and contact time (60 and 90 min). The surface area of the activated carbons and high removal efficiency of MB and AO7 was chosen as a measure of the optimization. The activated carbon prepared at 500 °C, for 3 hours with an H₃PO₄ concentration of 2.5 mol/L and a contact time of 90 min, have the largest specific surface area (475 m^2/g) and the percentage of discoloration of methylene blue (99.4%). Furthermore, the greater value of AO7 removal (94.20%) was obtained at 3h - activation time, 500°C - activation temperature, 1.5 mol/L - H₃PO₄ concentration with a 90 min contact time.

Keywords: *Cucumis melo*; activated carbon; H₃PO₄ activation; full factorial design; specific surface area; dyes.

1. Introduction

Textile dyes are frequently utilized in unlimited industrial applications such as textile, paint, printing, cosmetics, and food as a coloring agent [1]. The discharge of synthetic dyes without treatment into the aqueous environment is one of the most important environmental problems due to its risks on aquatic life and human health [2]. In the literature, numerous techniques have been employed and investigated extensively to remove dyes from wastewater. Activated carbons are very efficient and have been preferentially used for the adsorption of dyes, but their use is restricted due to high cost [3]. The preparation of a new activated carbon from a cheap and available source has proven useful [4,5].

Activated carbon (AC) is a long-known adsorbent characterized, among other things [6], by its large specific surface area and its porous structure [7,8]. It can be prepared from any solid matter containing a large proportion of carbon [9,10], often by carbonization followed

physical or chemical activation. However, a process combining the two stages can be applied. The main purpose of carbonization is to enrich the material with carbon and create the first pores, while activation aims to develop a porous structure [11].

The preparation of activated carbon from local biomass by the chemical activation method has been the subject of several studies [12-16]. The advantage of chemical activation is to operate at low pyrolysis temperatures and a lower activation cost. High quality activated carbon with a very large porous structure and large specific surface area is prepared by plant biomass using orthophosphoric acid as a chemical activating agent. Controlling the texture and porosity of activated carbon requires mastery of the steps in the process of synthesis of activated carbon by physical or chemical activation, by optimizing the steps of the preparation method.

For these reasons, the full factorial design (FFD) allows you to obtain the maximum amount of information with the minimum of experience [17,18]. It allows a complete study of the influence of all factors on the given process and their optimization. This by looking for a simple mathematical model giving a good representation of the phenomenon studied.

Through this work, our contribution in this area is to prepare activated carbon by chemical activation from the residues of *Cucumis melo* with orthophosphoric acid (H_3PO_4) as an activating agent. Then optimizing preparation parameters using FFD as a design technique by analyzing the effects of independent variables comprising activation time, activation temperature, the concentration of activating agent H_3PO_4, and contact time on the prepared activated carbon surface and the capacity of removing cationic and anionic dyes: Methylene blue (MB) and Acid orange 7 (AO7) from aqueous solution.

2. Materials and Methods

2.1. Preparation of optimized AC.

The adsorbent materials used in this study are activated carbons prepared by varying the preparation method's different parameters (Activation time, Activation temperature, the concentration of activating agent).

2.1.1. Purification.

The residues of Cucumis melo are food waste collected. They are thoroughly washed with tap water, then with distilled water, until the odor disappears and the rinse water is clear. Then they are dried for 24 hours at a temperature of 110 °C in an oven. They are then crushed and sieved to retain very fine particles, then washed several times with distilled water to remove impurities (dust and water-soluble substances), then dried at 110 °C for 24 h before undergoing chemical activation with phosphoric acid.

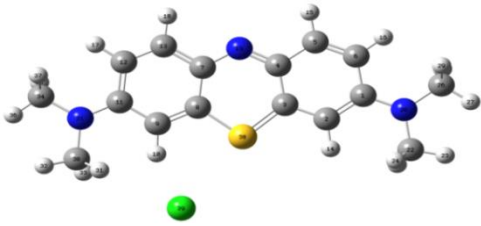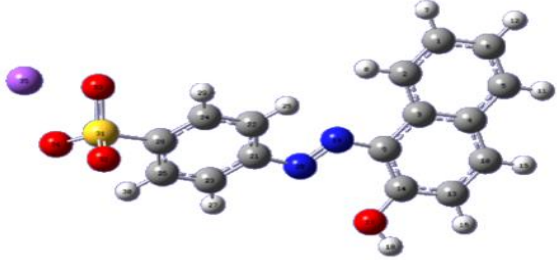#### 2.1.2. Chemical activation with phosphoric acid.

The retained particles are impregnated in a phosphoric acid solution with concentrations ranging from 1.5 to 2.5 mol / L. The impregnated particles are kept in hermetically sealed flasks until carbonization tests are carried out. The carbonization is carried out in an oven preheated to an adequate temperature before the experiment starts to obtain equilibrium. Carbonization is carried out at temperatures varying from 300 to 500 °C. and at times varying from 1 to 3 h. The coals obtained are cooled to room temperature in desiccators. The active charcoals are

washed in 0.1 M hydrochloric acid solutions to remove any carbonization residues and then rinsed several times with distilled water to constant pH. The coals thus washed and rinsed are dried at 105 °C for 24 h in an oven, then cooled in desiccators and stored away from air in tightly closed flasks until characterization tests.

2.2. Adsorbates.

Two dyes were chosen as the cationic and anionic dye models, MB and AO7, respectively. Table 1 shows the main characteristics of the used dyes.

Table 1. Some general characteristics of the used dyes [19].

Dye	Chemical structure	Molecular weight (g/mol)	λ_{max} (nm)
Methylene blue		319.86	663
Acid orange 7		350.32	485

The characterization of an activated carbon requires knowledge of its specific surface. This surface is generally determined by Brunauer, Emmet, and Teller's method, commonly known as the BET method. In our study, the determination of the specific surface was calculated using the Langmuir isotherm.

2.3. Batch adsorption study.

The adsorption tests were carried out in batch mode by shaking the dye's synthetic solutions in the presence of each of the active activated carbon. The solutions studied are prepared by successive dilutions of the stock solutions until the desired concentrations are obtained. The residual concentration of each of the dyes was determined using a UV/Visible spectrophotometer (Jenway 6300). The absorbance was measured after centrifugation at 1500 rpm for 2 min of the solution treated using a centrifuge.

The percent removal (%) of dyes was calculated using the following equation:

$$\% \text{ Removal dye} = \frac{C_0 - C_t}{C_0} * 100 \qquad (1)$$

Where, C_0 is the initial dye concentration and C_e (mg/L) is the concentrations of dye at equilibrium.

The amount of dye adsorption per unit mass of activated carbon at equilibrium, q_e (mg/g) was calculated by the following equation:

$$q_e \ (mg/g) = \frac{C_0 - C_e}{m} * V \tag{2}$$

Where, C_e (mg/L) is the liquid concentration of dye at equilibrium, C_0 (mg/L) is the initial concentration of dye in solution. V is the volume of the solution (L) and m is the mass of optimized activated carbon (g).

The Langmuir isotherm has been used to determine the specific surface area of biological and inorganic materials [20,21]. The specific surface area was calculated by the following equation [22]:

$$S_{MB} = \frac{Q_{max} * A_{MB} * N}{M_{MB}} \tag{3}$$

Where, S_{MB} (m^2/g) is the specific surface area; Q_{max} (mg/g) is the maximum adsorption capacity (calculated from the Langmuir isotherm); A_{MB} is the occupied surface area of one molecule of methylene blue = 197.2 $Å^2$ [23]. N is the Avogadro's number, 6.02×10^{23} and M is the molecular weight of MB (373.9 g/mol).

2.4. Design of experiment by FFD.

The factorial experimental design was used to optimize the preparation conditions of *Cucumis melo* activated carbon and treatment performance in terms of removing cationic (MB) and anionic (AO7) dye at the same time by adsorption.

This study chose four factors: the activation time, the activation temperature, the concentration of activating agent H_3PO_4, and the contact time. These factors are those which a priori have a direct influence on the process of preparation of activated carbon. The quality and effectiveness of our activated carbon prepared from *Cucumis melo* are determined by the measurement of the specific surface area and the percentage of elimination of the dyes studied: MB and AO7. That is to say, in the range of factors studied, an increase in the percentage of elimination of the dyes studied explains the increase in the quality of the activated carbon prepared (a large adsorption capacity, a large specific surface, pore development) and vice versa. The factors studied, accompanied by their range of variation, are given in Table 2.

Table 2. Experimental ranges and levels of the factors used in the factorial design.

Independent variable	Coded symbol	Range and level	
		-1	**+1**
Activation time (h)	A	1	3
Activation temperature (°C)	B	300	500
Concentration of H_3PO_4 (mol/L)	C	1.5	2.5
Contact time (min)	D	60	90

3. Results and Discussion

3.1. Experimental results.

Our study used a full factorial design model 2^n, where 2 represents the number of variation levels of each parameter and n = 4 the number of these parameters. The main factors of the full factorial plan (2^4) with 16 experiments carried out were studied with two levels chosen from the interval studied, a higher level (+) and a lower level (-). The mathematical relationship between the response (% R) and the four factors and their interaction were represented by the following regression equation:

R (%) = $X_0 + X_1$ A + X_2 B + X_3 C + X_4 D + X_5 AB + X_6 AC + X_7 AD + X_8 BC + X_9 BD + X_{10} CD + X_{11} ABC+ X_{12}ABD + X_{13} ACD +X_{14} BCD +X_{15}ABCD $\tag{4}$

Where, R represents the answer, in our case, it is the specific surface area of activated carbon and the percentage of elimination of MB and AO7, X_0 is the global mean, X_i represents the other regression coefficients, X_{ij} represents the effects of the interaction between the main factors and A, B, C, D stands for a time of activation, the temperature of activation, H_3PO_4 concentration and contact time, respectively.

The experimental results' processing will also make it possible to develop statistical, mathematical models giving the adsorption yield and the specific surface under the operating conditions studied. The coefficients of the main factors, their interactions, and their contribution percentages in the mathematical model developed are shown in Table 3.

Table 3. Values of model coefficients and percentage contribution of the three responses.

Main coefficients	SS (m^2/g)		MB (%)		AO7 (%)	
	Coefficient	% Contribution	Coefficient	% Contribution	Coefficient	% Contribution
X_0	387.8	–	86.02	–	67.94	–
X_1	49.80	31.74	8.534	37.95	8.921	14.93
X_2	49.41	31.24	6.713	23.48	15.24	43.58
X_3	16.50	3.48	4.883	12.42	9.843	18.17
X_4	30.55	11.95	- 1.924	1.929	6.896	8.923
X_{12}	- 16.34	3.41	- 4.781	11.90	0.792	0.117
X_{13}	- 14.09	2.54	- 0.215	0.024	- 4.334	3.524
X_{14}	- 0.380	0.001	- 0.239	0.029	- 1.467	0.404
X_{23}	16.16	3.34	1.518	1.201	- 4.541	3.869
X_{24}	- 27.15	9.43	- 1.351	0.950	- 4.130	3.200
X_{34}	0.527	0.003	- 1.243	0.805	1.389	0.361
X_{123}	- 13.98	2.50	- 3.293	5.651	- 2.988	1.674
X_{124}	-0.719	0.006	2.028	2.143	- 1.004	0.189
X_{134}	- 0.576	0.004	- 0.364	0.069	- 0.777	0.113
X_{234}	1.173	0.01	0.739	0.284	- 1.862	0.650
X_{1234}	- 4.841	0.30	- 1.474	1.132	1.201	0.270

By substituting the regression coefficients obtained in equation (4) by their numerical values given in Table 3, we obtain equations (5), (6), and (7) describing the specific surface of the activated carbon prepared and the adsorption efficiency of MB and AO7, respectively:

SS (m^2/g) = 387.8 + 49.80 A + 49.41 B + 16.50 C + 30.55 D – 16.34 A*B – 14.09 A*C –0.3803 A*D + 16.16 B*C – 27.15 B*D + 0.5274 C*D – 13.98 A*B*C + 0.7198 A*B*D – 0.5766 A*C*D + 1.173 B*C*D – 4.841 A*B*C*D   **(5)**

MB(%)= 86.02 + 8.534 A + 6.713 B + 4.883 C + 1.924 D – 4.781 A*B – 0.2156 A*C – 0.2394 A*D + 1.518 B*C – 1.351 B*D – 1.243 C*D – 3.293 A*B*C + 2.028 A*B*D – 0.3644 A*C*D + 0.7394 B*C*D – 1.474 A*B*C*D   **(6)**

AO7 (%)= 67.94 + 8.921 A + 15.24 B + 9.843 C + 6.896 D + 0.7925 A*B – 4.334 A*C – 1.467 A*D - 4.541 B*C- 4.130 B*D+ 1.389 C*D- 2.988 A*B*C - 1.004 A*B*D - 0.7775 A*C*D - 1.862 B*C*D + 1.201 A*B*C*D   **(7)**

3.2. Process optimization.

The preparation conditions and the experimental results of the three responses, the specific surface area of the activated carbon prepared, and the percentage of discoloration of MB and AO7 are illustrated in Table 4.

Table 4. Factorial design matrix of four variables and experimental and predicted responses for SS, MB, and AO7.

Run Nº	Coded values of independent variables				Responses (%)		
	A	B	C	D	SS (m^2/g)	MB (%)	AO7 (%)
1	-1	-1	-1	-1	208.1	57.07	22.58
2	+1	-1	-1	-1	351.3	84.3	38.5
3	-1	+1	-1	-1	347.	81.62	54.71
4	+1	+1	-1	-1	458.6	88.89	94.57
5	-1	-1	+1	-1	218.8	63.83	43.58
6	+1	-1	+1	-1	344.5	98.93	62.03
7	-1	+1	+1	-1	454.3	98.77	81.75
8	+1	+1	+1	-1	475.2	99.36	90.63
9	- 1	- 1	- 1	+1	335.5	74.34	35.1
10	+1	- 1	- 1	+1	457.3	88.06	57.08
11	- 1	+1	- 1	+1	338.9	76.52	66.98
12	+1	+1	- 1	+1	473.5	98.3	95.26
13	- 1	- 1	+1	+1	326.6	68.73	77.02
14	+1	- 1	+1	+1	464.9	99.2	85.7
15	- 1	+1	+1	+1	474.6	99.01	90.43
16	+1	+1	+1	+1	475.3	99.4	91.12

According to this table, it can be seen that the specific surface area of the activated carbon prepared varies between 208.1 m^2/g to 475.3 m^2/g, as well as the percentage of elimination varies between 57.07% to 99.4% for MB and between 22.58% to 95.26% for the AO7. These large variations in the percentage of elimination and the specific surface area confirm the significant influence of activation time, activation temperature, the concentration of H_3PO_4 activating agent, and the contact time on the quality of the specific surface area of the activated carbon prepares and consequently on the dye adsorption process.

The specific surface area and the porosities developed during the activation process allow the elimination of MB and AO7. Ineffective coals are those which have a relatively small specific surface and very few surface functions. According to these results, we see that our activated carbon prepares for test number 16 and 12 for the discoloration of MB and AO7, respectively, were having a large specific surface and a significant adsorption capacity compared to other activated carbon.

3.3. Statistical analysis.

In this study, to assess the importance of the regression model and find the relationship between the factors and the responses, an analysis of variance (ANOVA) was applied at a confidence level of 95% ($p < 0.05$) [24] for SS, MB, and AO7 and the results are grouped in Tables 5a, 5b, and 5c, respectively, by their degrees of freedom, the sum of squares, mean of squares, F-value, and P-value. Statistically significant values were determined by P-values. Model terms with P-values> 0.05 are considered statistically insignificant, while those with P-values <0.05 are considered statistically significant. Consequently, some coefficients in equations (5), (6), and (7) are negligible; the final empirical forms of the model for the three responses become equations (8), (9), and (10).

3.3.1. Specific surface (SS).

The results of the analysis of variance ANOVA show that the coefficients of activation time (A), activation temperature (B), contact time (D), the concentration of H_3PO_4 (C), and the

interaction between the activation temperature and the concentration of H_3PO_4 (BC) are positive. Therefore, these factors positively influence the quality of the specific surface area of the activated carbon prepared. The other remaining interactions (AB, AC, BD, and ABC) have negative coefficients (Eq. (8), Table 5). Therefore, their influence on the specific surface area is negative; that is to say, an increase in these interactions leads to a decrease in the activated carbon's specific surface area.

$$\text{SS } (m^2/g) = 387.81 + 49.8\ A + 49.41\ B + 16.5\ C + 30.55\ D - 16.34\ AB - 14.09\ AC + 16.16\ BC - 27.15\ BD - 13.98ABC \tag{8}$$

Table 5. Analysis of variance of specific surface area.

Source	Sum of Squares	df	Mean Square	F-value	P-value	Prob> F
Model	1.246E+05	9	13841.38	198.98	< 0.0001	significant
A-Time of activation	39679.82	1	39679.82	570.44	< 0.0001	
B-Temperature of activation	39054.05	1	39054.05	561.44	< 0.0001	
C- H_3PO_4 Concentration	4357.66	1	4357.66	62.65	0.0002	
D- Contact time	14937.71	1	14937.71	214.74	< 0.0001	
AB	4271.14	1	4271.14	61.40	0.0002	
AC	3176.96	1	3176.96	45.67	0.0005	
BC	4179.29	1	4179.29	60.08	0.0002	
BD	11789.80	1	11789.80	169.49	< 0.0001	
ABC	3125.99	1	3125.99	44.94	0.0005	
Residual	417.36	6	69.56			
Cor Total	1.250E+05	15				

3.3.2. Methylene blue (MB).

According to the analysis of variance ANOVA for the response of the adsorption efficiency of MB, it can be concluded that the most significant factors are: activation time (A), activation temperature (B), and the concentration of the activating agent H_3PO_4 (C) and the interaction between the activation time (A) and the activation temperature (B) (Eq. (9), Table 6).

$$\text{MB } (\%) = 86.02 + 8.53\ A + 6.71\ B + 4.88\ C - 4.78\ AB \tag{9}$$

Table 6. Analysis of variance of MB.

Source	Sum of Squares	df	Mean Square	F-value	P-value	Prob> F
Model	2633.61	4	658.40	16.59	0.0001	significant
A-Time of activation	1165.37	1	1165.37	29.36	0.0002	
B-Temperature of activation	721.06	1	721.06	18.16	0.0013	
C- H_3PO_4 Concentration	381.52	1	381.52	9.61	0.0101	
AB	365.67	1	365.67	9.21	0.0113	
Residual	436.68	11	39.70			
Cor Total	3070.29	15				

3.3.3. Acid orange 7 (AO7).

Similarly, according to the analysis of variance ANOVA of the adsorption efficiency of AO7, the significant effects are the four factors A, B, C, and D and their interaction AC, BC, and BD (Eq. (10), Table 7).

$$\text{AO7 } (\%) = 67.94 + 8.92\ A + 15.24\ B + 9.84\ C + 6.90\ D - 4.33\ AC - 4.54\ BC - 4.13\ BD \tag{10}$$

Table 7. Analysis of variance of AO7.

Source	Sum of Squares	df	Mean Square	F-value	P-value	Prob> F
Model	8204.46	7	1172.07	29.07	< 0.0001	significant
A-Time of activation	1273.42	1	1273.42	31.58	0.0005	
B-Temperature of activation	3716.73	1	3716.73	92.18	< 0.0001	
C- H_3PO_4 Concentration	1550.00	1	1550.00	38.44	0.0003	
D- Contact time	760.93	1	760.93	18.87	0.0025	
AC	300.50	1	300.50	7.45	0.0258	
BC	329.97	1	329.97	8.18	0.0211	
BD	272.91	1	272.91	6.77	0.0315	
Residual	322.55	8	40.32			
Cor Total	8527.01	15				

3.4. Diagnostic model.

In order to test the quality of the fit of the model, statistical data such as F-value, P-value, coefficient of correlation (R^2), adjusted R^2, coefficients of variance (CV), and adequate precision were examined. A P-value of less than 0.05 demonstrates the factor effect's statistical significance (at a 95% confidence level). According to the results of the analysis of variance ANOVA (Table 5-7), the F values of the model with a very low probability value ($p < 0.0001$) were determined at 198.9, 16.59, and 29.07 for SS, MB, and AO7, respectively, indicating that the three models were significant. The high values of the correlation coefficient (R^2) and adjusted R^2 (0.9967 and 0.9917 for SS, 0.8578 and 0.8061 for MB and 0.9622 and 0.9291 for AO7, which are greater than 0.80 confirm and suggest that the model has high efficiency for the representation of experimental data (Table 8 and Fig. 1a-c) [25,26].

Table 8. R^2, SD, CV, and AP values of the model equations for SS, MB, and AO7.

Response	R^2	Adj R^2	Pred R^2	SD	CV (%)	AP
SS	0.9967	0.9917	0.9763	8.34	2.15	40.12
MB	0.8578	0.8061	0.8578	6.30	7.32	11.43
AO7	0.9622	0.9291	0.8487	6.35	9.25	18.22

Figures 1a-c show the correlation between the experimental values and the predicted values of SS, MB, and AO7, respectively. We could see that in the three responses, the scattering between the data points and the diagonal line showed an adequate agreement between the real and predicted data obtained by the model.

On the other hand, the coefficient of variance (CV) is the standard deviation ratio to the mean expressed as a percentage. The higher the coefficient of variation, the greater the level of dispersion around the mean. It is generally expressed as a percentage. A model can be generally considered reliable if it's CV <10% [27]. According to Table 8, the CV values for the specific surface (SS) and the percentage of discoloration of MB and AO7 were found to be 2.15%, 7.32%, and 9.35%. These low values de CV clearly show that the difference between the experimental and predicted values is small and also confirms the reliability of the models developed [28].

Figure 1. Actual versus predicted data of (**a**) SS; (**b**) MB; (**c**) AO7.
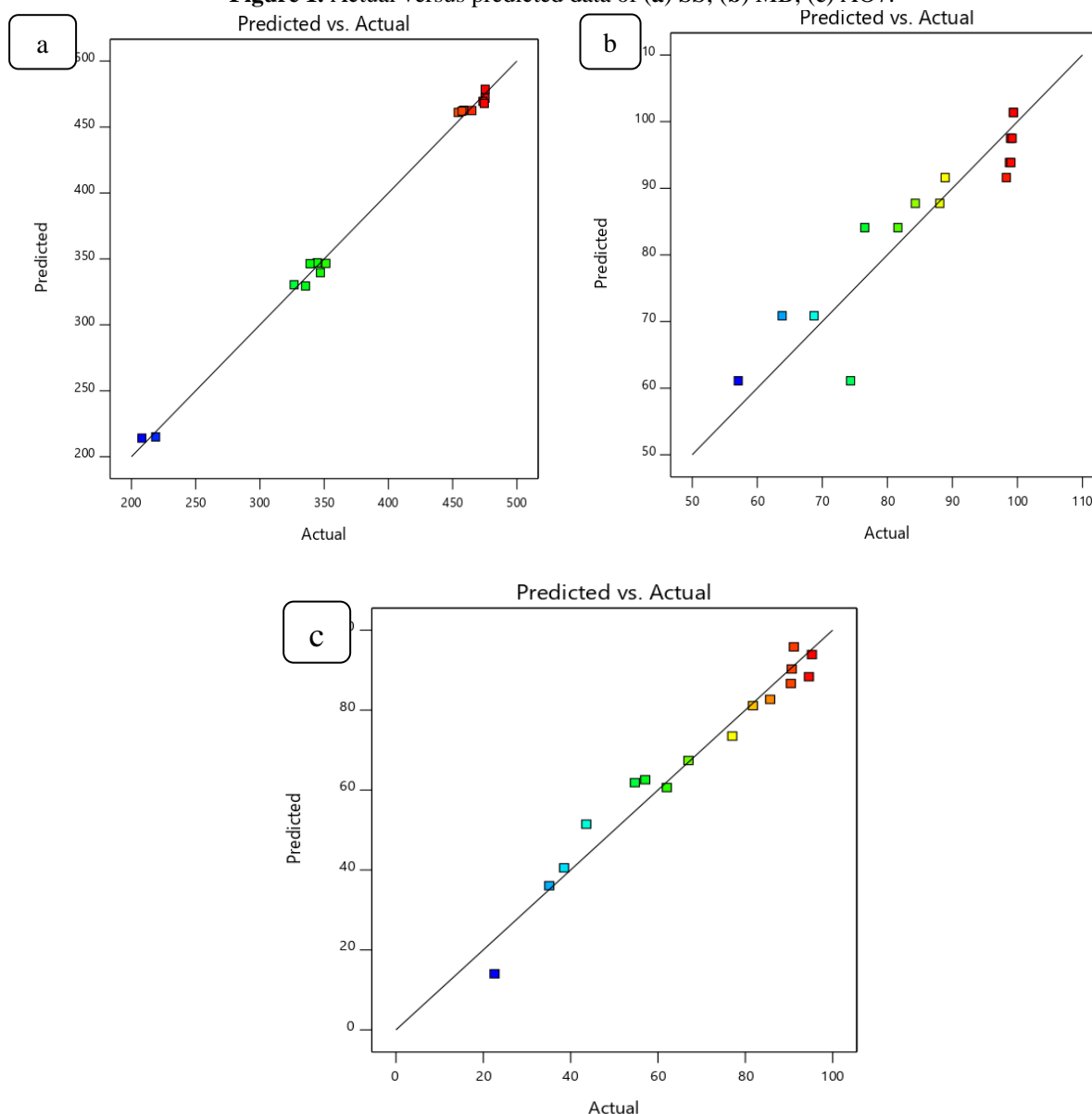
3.5. Adequacy of prediction models.

Adequate accuracy measures the signal-to-noise ratio and compares the range of values predicted at design points to the average prediction error. A ratio greater than 4 is desirable and indicates adequate model discrimination. In the present study, the adequate and higher precision value of the order of 40.12, 11.43, and 18.22 for SS, MB, and AO7, respectively, show a good agreement on the experiments' reliability performed [29].

The results in Table 9 allow a more precise assessment of the quality of the adjustment made. The comparison between the columns $R_{observed}$ (measured responses) and $R_{Predicted}$ (responses predicted by the model) confirms that the fit is good. The adjusted (predicted) values are included in the respective confidence intervals (CI), which validates the experimental design model with linear regression coefficients R^2 of 99.67%, 85.78% and 96.22% for SS, MB, and AO7, respectively.
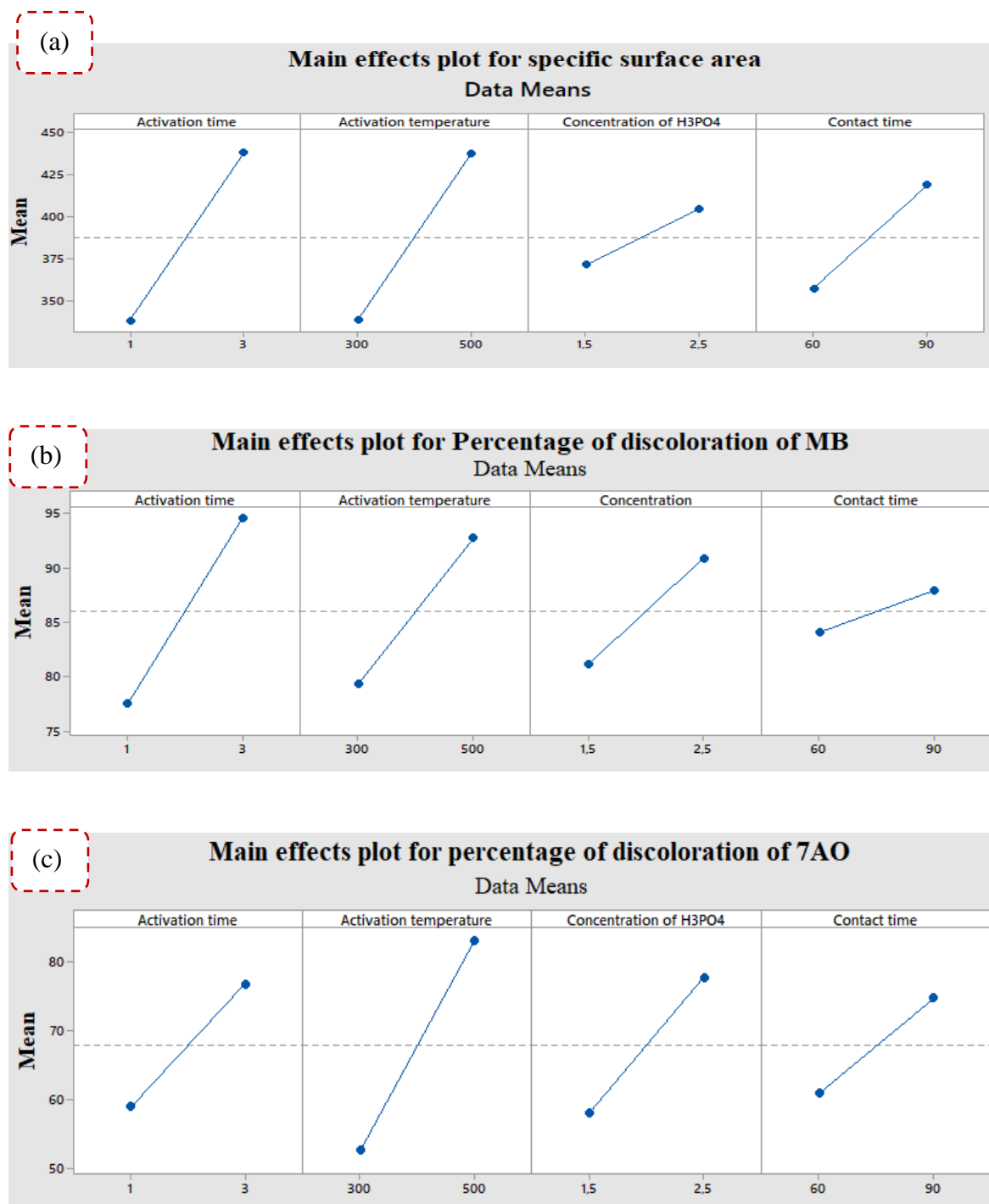
Figure 2. (**a**) Main effects plot on the specific surface area; the percentage of discoloration of (**b**) MB; (**c**) AO7.

Table 9. Factorial design matrix of four variables and experimental and predicted responses for SS, MB, and AO7.

Run Nº	SS (m²/g)			MB (%)			AO7 (%)		
	Observed	Predicted	Residual	Observed	Predicted	Residual	Observed	Predicted	Residual
1	208.1	214.1	-6.01	57.07	61.11	-4.04	22.58	14.03	8.55
2	351.3	346.6	4.72	84.3	87.74	-3.44	38.50	40.54	-2.04
3	347.	339.6	7.46	81.62	84.10	-2.48	54.71	61.86	-7.15
4	458.6	462.6	-4.72	88.89	91.60	-2.71	94.57	88.37	6.20
5	218.8	215	3.81	63.83	70.88	-7.05	43.58	51.47	-7.89
6	344.5	347	-2.52	98.93	97.51	1.42	62.03	60.64	1.39
7	454.3	461	-6.78	98.77	93.86	4.91	81.75	81.13	0.62
8	475.2	471.2	3.38	99.36	101.3	-2.01	90.63	90.30	0.33
9	335.5	329.5	6.01	74.34	61.11	13.23	35.10	36.09	-0.98

Run N°	SS (m²/g)			MB (%)			AO7 (%)		
	Observed	Predicted	Residual	Observed	Predicted	Residual	Observed	Predicted	Residual
10	457.3	462.02	-4.72	88.06	87.74	0.32	57.08	62.60	-5.52
11	338.9	346.4	-7.46	76.52	84.10	-7.58	66.98	67.39	-0.41
12	473.5	469.4	4.06	98.30	91.60	6.70	95.26	93.90	1.36
13	326.6	330.4	-3.81	68.73	70.88	-2.15	77.02	73.52	3.50
14	464.9	462.3	2.52	99.20	97.51	1.69	85.70	82.70	3.00
15	474.6	467.9	6.78	99.01	93.86	5.15	90.43	86.66	3.77
16	475.3	478.7	-3.38	99.40	101.37	-1.97	91.12	95.84	-4.72

3.6. Effects of the main factors.

The preparation of high quality activated carbon was evaluated based on high values of the specific surface area and the percentage of discoloration (%) of MB and AO7. Figures 2a-c show the effect of each factor on the response. These figures show that the activation temperature and the activation time have the greatest influence on the percentage of discoloration of MB and AO7 and on the specific surface area of the activated carbon prepared, followed by the activating agent's concentration. However, the contact time does not affect the percentage of discoloration of MB. The increase in the activation temperature from 300 ° C to 500 ° C leads to an opening and a widening of the pores, which increases the specific surface and the adsorption efficiency of MB and AO7 on the activated carbon prepared [30].

Indeed, when the activation time varies between 1 to 3 h, the microporosity increases, which gives activated carbon a better percentage of discoloration of MB and AO7 due to better development of their porosity and their specific surface areas. In the same way, it can be deduced that the concentration of H_3PO_4 has a significant influence on the percentage of discoloration of AO7, while an increase in the concentration of the activating agent H_3PO_4 from 1.5 M to 2.5 M promotes the development of pores on the surface of prepared activated carbon. However, chemical activation with H_3PO_4 made it possible to obtain activated carbon with a well-developed mesoporosity, which is favorable for adsorbing larger molecules such as MB and AO7.

3.7. 3D surfaces and 2D contour plots.

To assess the effects of variables, the 3D surfaces and 2D contour plots are demonstrated for a function of two factors. This representation shows the relative effects of any two variables when the remaining variables are kept constant. Figures 3 and 4 show the plots of the three-dimensional response surfaces (3D) and the contour curves (2D) constructed to present the significant interactions. According to these figures, we notice on the surfaces response (a,b) and the contour curves (c,d) of Figure 3, that the best specific surface area (475.3 m²/g) and percentage discoloration of AO7 (95.26%) are obtained when working with maximum values of A*C, B*C and B*D.

Similarly, by analyzing Figure 4 (e,f) of the MB, it can be deduced that the activation time and the activation temperature have an important influence on the percentage discoloration of the MB with a percentage discoloration of 99.4%.
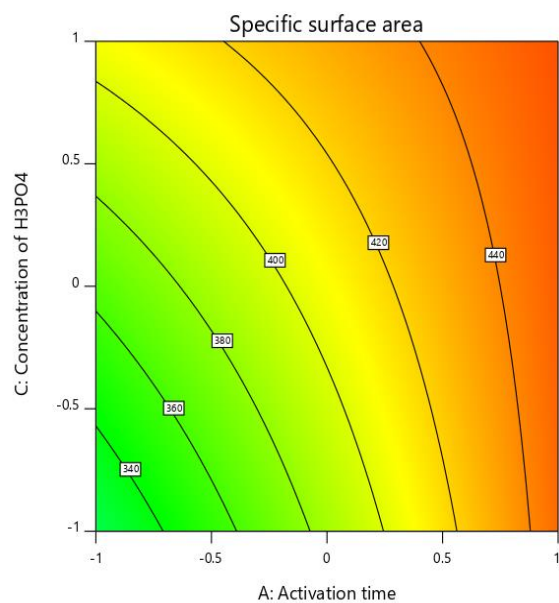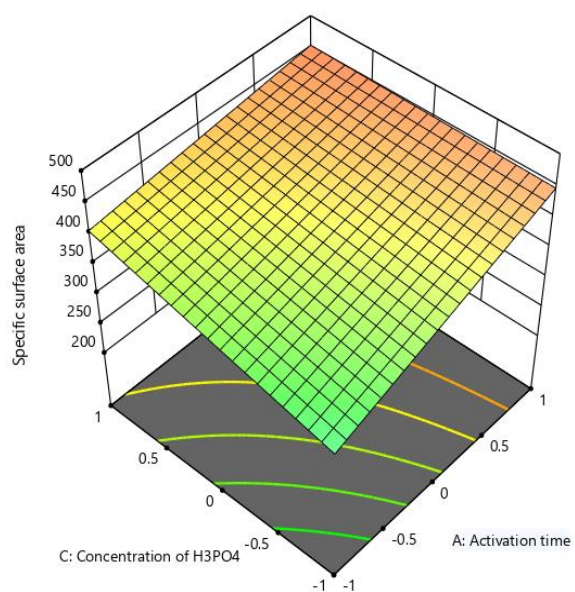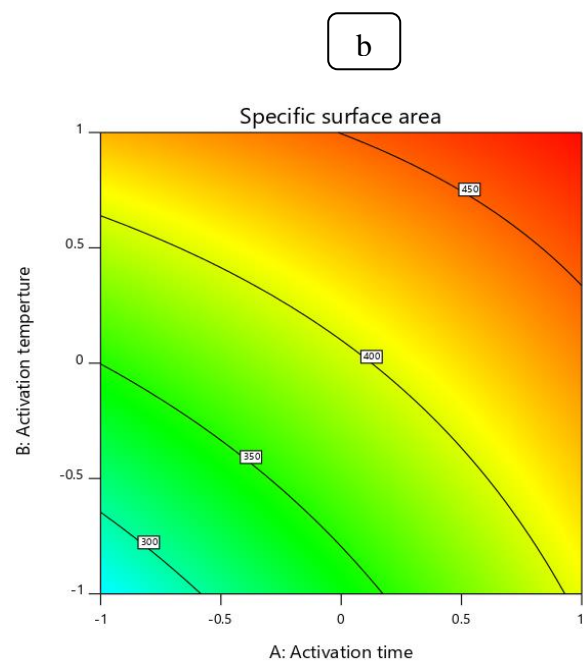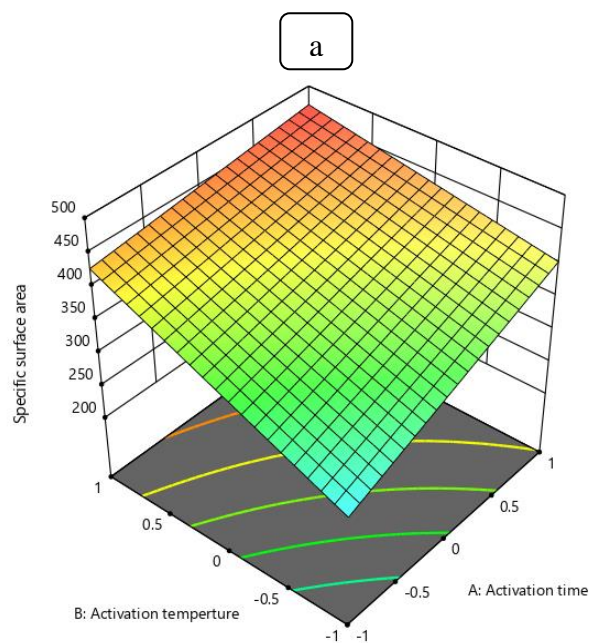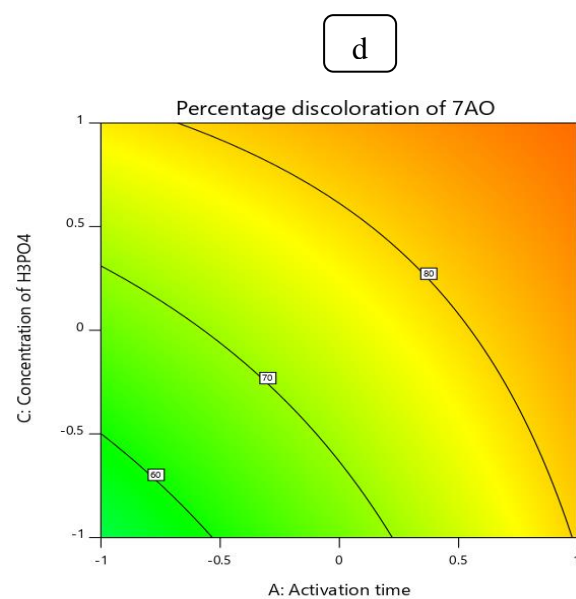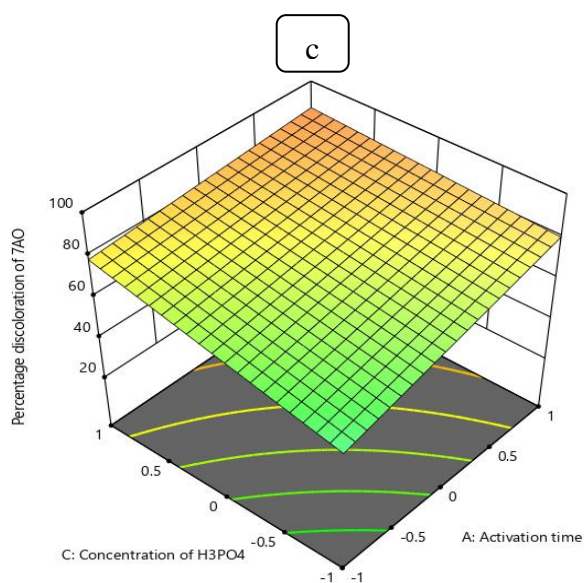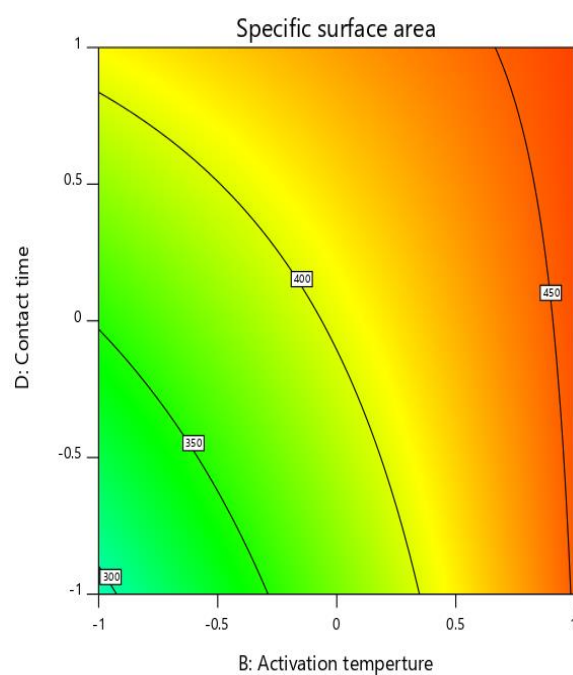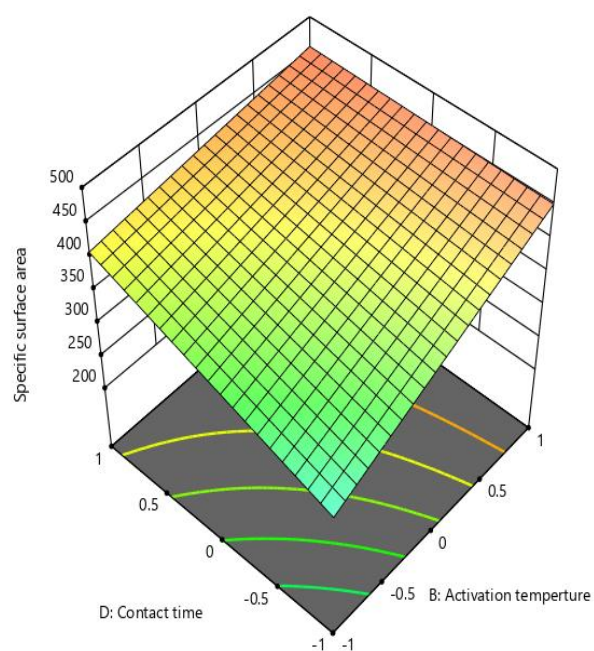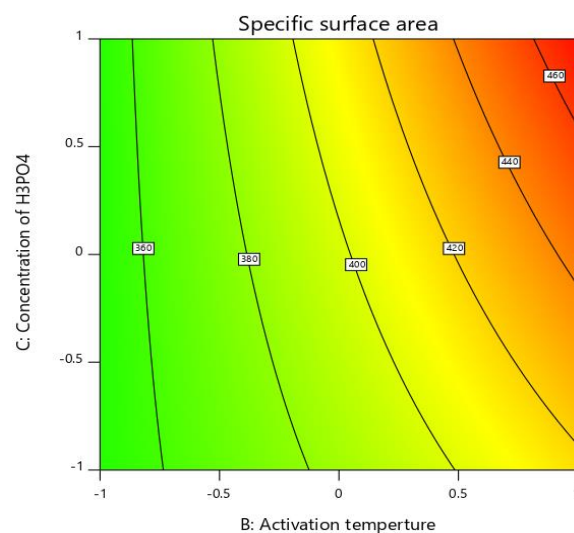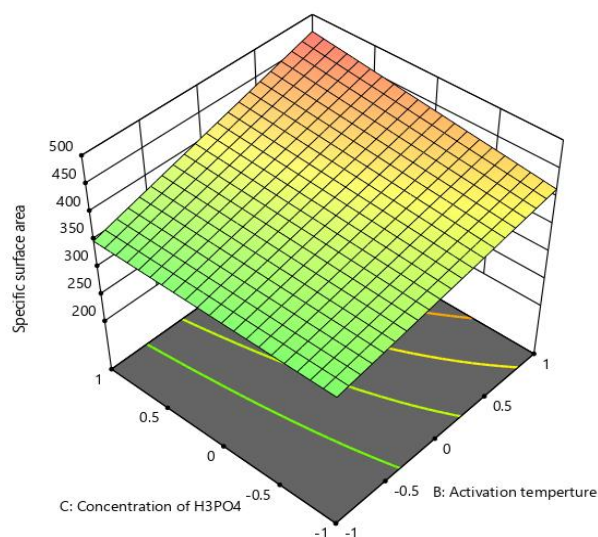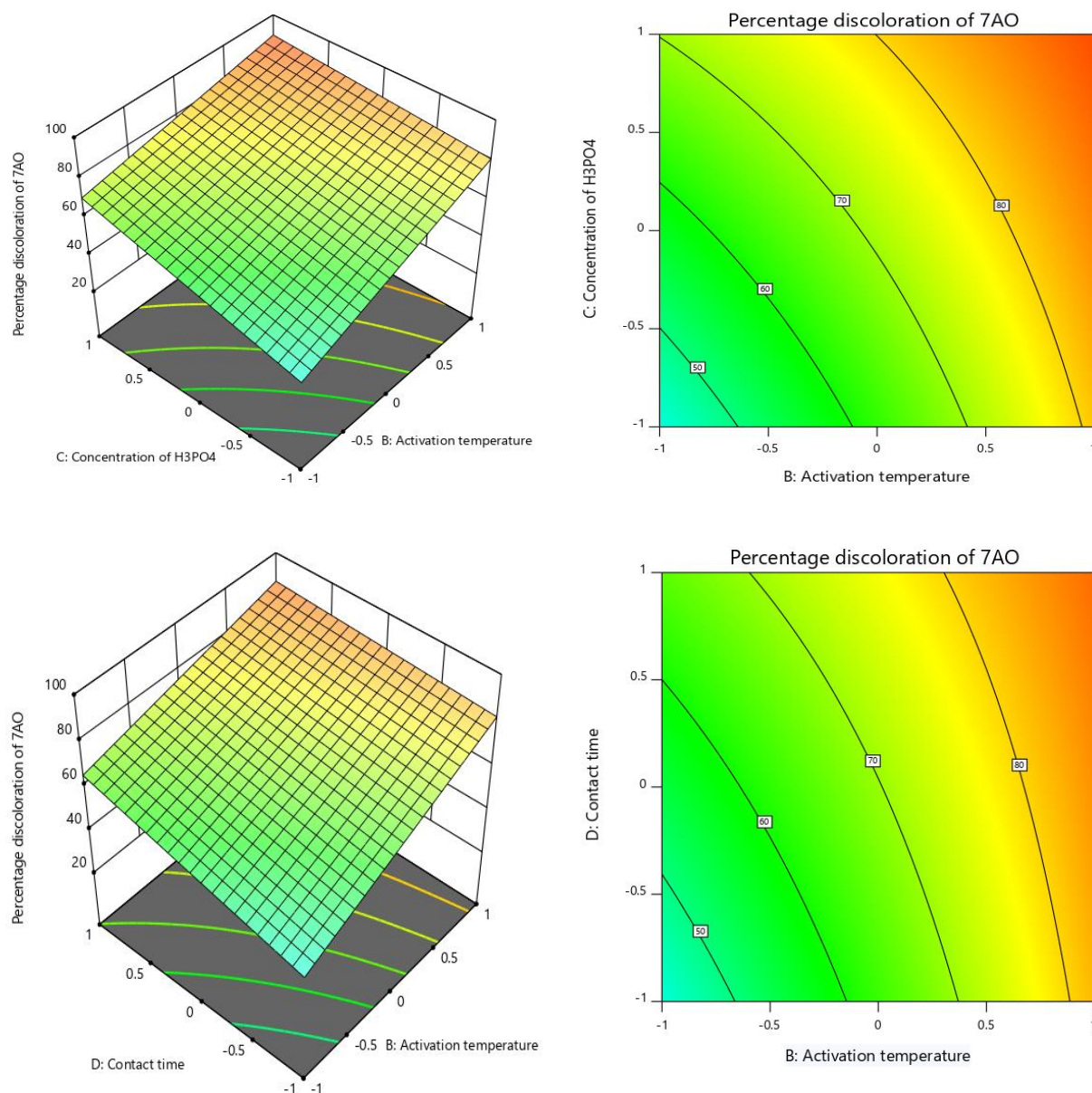
Figure 3. Surface response and contour plots for (**a,b**) specific surface area; (**c,d**) AO7.
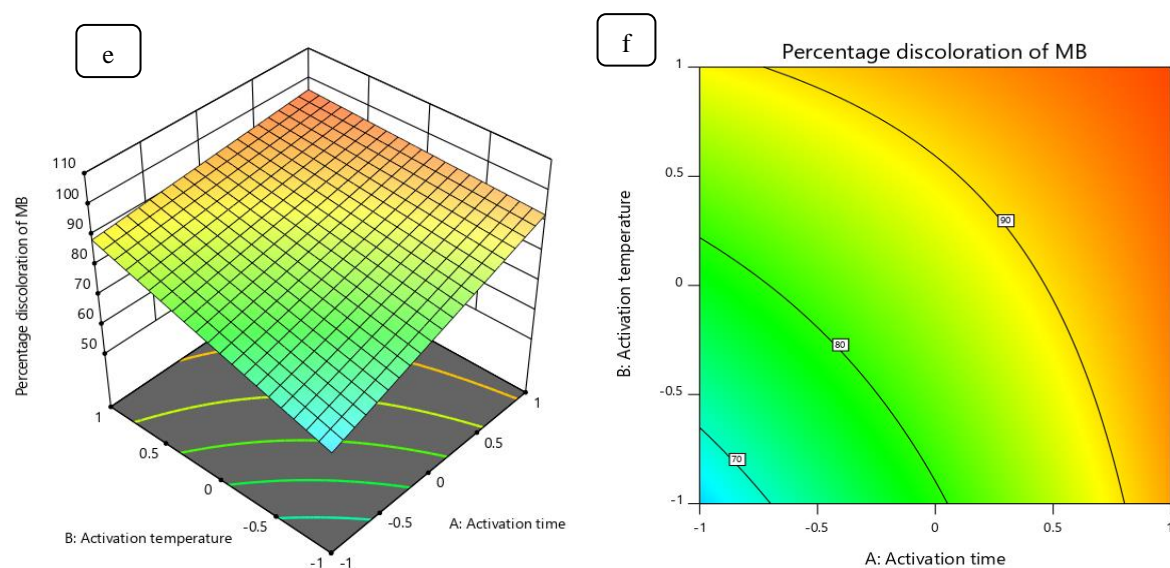

Figure 4. Surface response and contour plots for the (**a,b**) MB.

3.8. Characterization of optimized AC.

3.8.1. FTIR analysis.

Fourier-transform infrared spectroscopy (FTIR) analysis was applied to determine the functional groups present on the prepared activated carbon surface and understand the adsorption mechanism [31]. The infrared spectrum has been recorded from 400 to 4000 cm^{-1} is represented in Figure 5. The analysis of these spectra makes it possible to cite the following characteristic bands. A wide absorption band was observed at 3410 cm^{-1} and 3408 cm^{-1} correspondingly to the hydroxyl groups' elongation. This band indicates the presence of carboxyl groups, phenols, or alcohols linked to water adsorbed on the surface of activated carbon [32]. The bands observed at 2922 cm^{-1} and 2852 cm^{-1} are absorption bands attributed to the asymmetric and symmetrical valence vibration of the –CH$_3$ and CH$_2$ groups. A band around 1300 -1000 cm^{-1} corresponds to the C– O bond of phenols, carboxylic acids, and esters or the P = O bond of ester phosphates, or the O – C bond of P – O – C [33]. This band is also characteristic of phosphorus and phosphocarbon compounds present in activated carbon achieving by phosphoric acid. The spectrum also shows a peak at 520 cm^{-1} that could be attributed to the P-O stretching vibration and/or aromatic structures. This indicates that these functional groups could act as active sites for interaction with dye molecules [34].
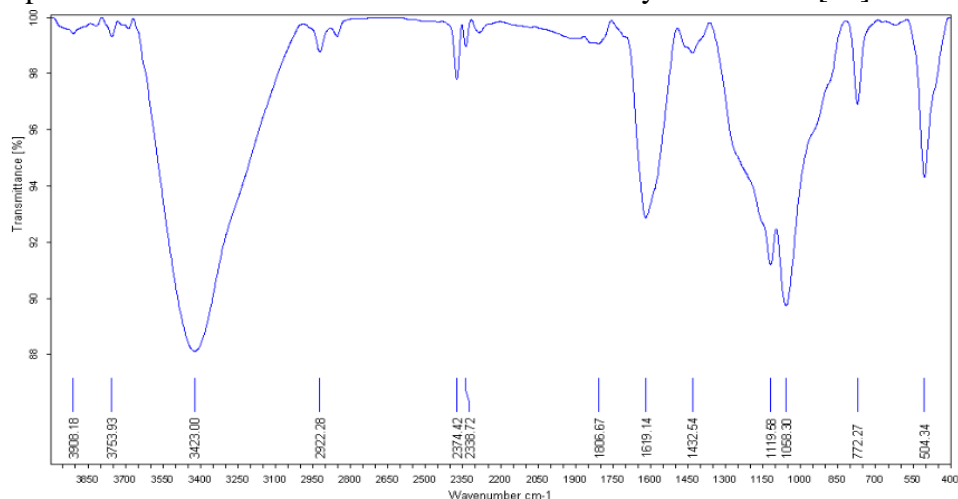

Figure 5. FT-IR spectra of *Cucumis melo* activated carbon.

3.8.2. SEM analysis.

Figure 6 presents an SEM image before and after adsorption. This image clearly shows a wide distribution of pores of different shapes and sizes before adsorption (Figure 6a). However, the SEM image analysis in Figure 6b shows that the activated carbon's surface is much more homogeneous and saturated after adsorption. This means that there is a filling of the pores and active sites by the dye's adsorption on the prepared activated carbon's surface.
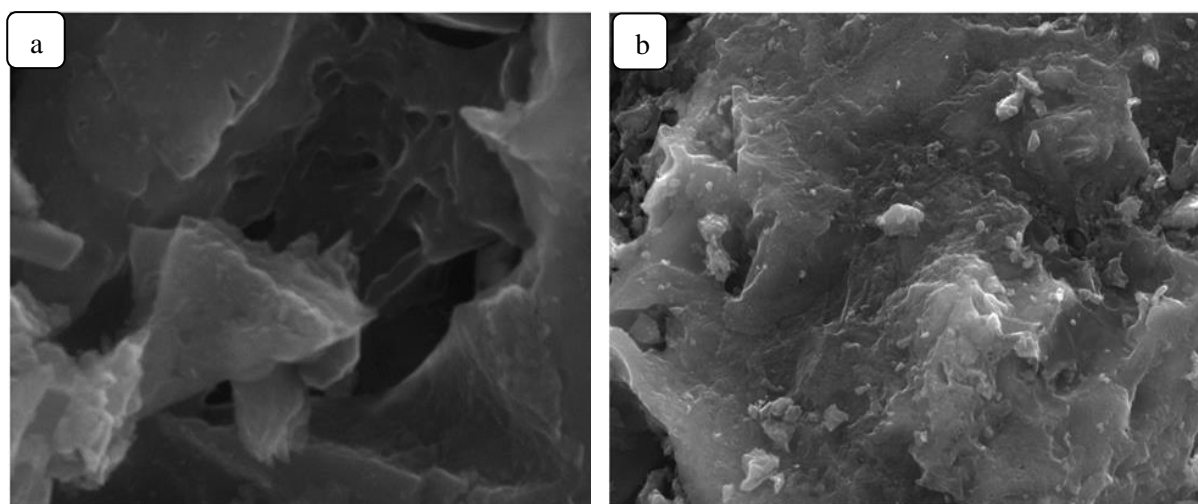
Figure 6. Scanning electron microscopic images of *Cucumis melo* activated carbon before and after adsorption.

4. Conclusions

In this study, activated carbon with a large specific surface area and a high removal efficiency of dye were prepared from *Cucumis melo* using H_3PO_4 as an activating agent. The conditions for preparing activated carbon by chemical activation were first optimized using a full factorial design with four factors: the activation time, the activation temperature, the concentration of H_3PO_4, and the contact time. The influence of the different factors on the yield and the adsorption capacity measured by the specific surface area and of the percentage of discoloration of MB and AO7 could be modeled satisfactorily.

The best result of specific surface area and MB is 475.3 m^2/g and 99.4%, respectively, were found at optimum process conditions, i.e., activation time (3h), activation temperature (500 °C), H_3PO_4 concentration (2.5 mol/L), and Contact time (90 min). However, the best value for the percentage of discoloration of AO7 (95.26%) was identified at an activation time of 3h, an activation temperature of 500 °C, and an H_3PO_4 concentration of 1.5 mol/L with 90 min contact time.

Conflicts of Interest

The authors declare no conflict of interest.

References

1. Anuar, F.I.; Hadibarata, T.; Syafrudin, M.; Fona, Z. Removal of Procion Red MX- 5B from aqueous solution by adsorption on Parkia speciosa (stink bean) peel powder. *Biointerface Res. Appl. Chem.* **2020**, *10*, 4774–4779, https://doi.org/10.33263/BRIAC101.774779.
2. Abdulhameeda, A.S.; Mohammada, A.-T.; Jawadb, A.H. Modeling and mechanism of reactive orange 16 dye adsorption by chitosan-glyoxal/TiO2 nanocomposite: application of response surface methodology. *Desalination and. Water Treatment* **2019**, *164*, 346-360, https://doi.org/10.5004/dwt.2019.24384.

3. Katheresan, V.; Kansedo, J.; Lau, S.Y. Efficiency of various recent wastewater dye removal methods: A review. *Journal of Environmental Chemical Engineering* **2018**, *6*, 4676-4697, https://doi.org/10.1016/j.jece.2018.06.060.

4. Achary, P.G.R.; Ghosh, M.R.; Mishra, S.P. Insights into the modeling and application of some low cost adsorbents towards Cr(VI) adsorption. *Materials Today: Proceedings* **2020**, *30*, 267-273, https://doi.org/10.1016/j.matpr.2020.01.433.

5. Choi, H.-J.; Yu, S.-W. Biosorption of methylene blue from aqueous solution by agricultural bioadsorbent corncob. *Environmental Engineering Research* **2019**, *24*, 99-106, https://doi.org/10.4491/eer.2018.107.

6. El Kassimi, A.; Boutouil, A.; El Himri, M.; Rachid Laamari, M.; El Haddad, M. Selective and competitive removal of three basic dyes from single, binary and ternary systems in aqueous solutions: A combined experimental and theoretical study. *Journal of Saudi Chemical Society* **2020**, *24*, 527-544, https://doi.org/10.1016/j.jscs.2020.05.005.

7. Kristanti, R.A.; Hadibarata, T.; Al Qahtani, H.M.A. Adsorption of bisphenol A on oil palm biomass activated carbon: characterization, isotherm, kinetic and thermodynamic studies. *Biointerface Research in Applied Chemistry* **2019***, 9*, 4217-4224, https://doi.org/10.33263/BRIAC95.217224.

8. Shabaan, O.A.; Jahin, H.S.; Mohamed, G.G. Removal of anionic and cationic dyes from wastewater by adsorption using multiwall carbon nanotubes. *Arabian Journal of Chemistry* **2020**, *13*, 4797-4810, https://doi.org/10.1016/j.arabjc.2020.01.010.

9. Kanthasamy, S.; Hadibarata, T.; Hidayat, T.; Alamri, S.A.; Ahmed al-Ghamdi, A. Adsorption of azo and anthraquinone dye by using watermelon peel powder and corn peel powder: Equilibrium and kinetic studies. *Biointerface Res. Appl. Chem.* **2020**, *10*, 4706–4713, https://doi.org/10.33263/BRIAC101.706713.

10. Kuang, Y.; Zhang, X.; Zhou, S. Adsorption of methylene blue in water onto activated carbon by surfactant modification. *Water* **2020**, *12*, 587, https://doi.org/10.3390/w12020587.

11. Saleem, J.; Shahid, U.B.; Hijab, M.; Mackey, H.; McKay, G. Production and applications of activated carbons as adsorbents from olive stones. *Biomass Conversion and Biorefinery* **2019**, *9*, 775-802, https://doi.org/10.1007/s13399-019-00473-7.

12. Ani, J.U.; Akpomie, K.G.; Okoro, U.C.; Aneke, L.E.; Onukwuli, O.D.; Ujam, O.T. Potentials of activated carbon produced from biomass materials for sequestration of dyes, heavy metals, and crude oil components from aqueous environment. *Applied Water Science* **2020**, *10*, 69, https://doi.org/10.1007/s13201-020-1149-8.

13. Heidarinejad, Z.; Dehghani, M.H.; Heidari, M.; Javedan, G.; Ali, P.I.; Sillanpää, M. Methods for preparation and activation of activated carbon: a review. *Environ. Chem. Lett.* **2020**, *18*, 1-23, https://doi.org/10.1007/s10311-019-00955-0.

14. Aziz, E.K.; Abdelmajid, R.; Rachid, L.M.; Mohammadine, E.H. Adsorptive removal of anionic dye from aqueous solutions using powdered and calcined vegetables wastes as low-cost adsorbent. *Arab Journal of Basic and Applied Sciences* **2018**, *25*, 93-102, https://doi.org/10.1080/25765299.2018.1517861.

15. Jawad, A.H.; Rashid, R.A.; Ishak, M.A.M.; Ismail, K. Adsorptive removal of methylene blue by chemically treated cellulosic waste banana (Musa sapientum) peels. *Journal of Taibah University for Science* **2018**, *12*, 809-819, https://doi.org/10.1080/16583655.2018.1519893.

16. Moughaoui, F. ; Ouaket, A. ; Laaraibi, A. ; Hamdouch, S. ; Anbaoui, Z. ; Abourriche, A.; Berrada, M. A novel approach for producing low cost and highly efficient activated carbon for removing cationic dyes. *Mediterranean Journal of Chemistry.*, **2019**, *8*(2), 74-83, http://dx.doi.org/10.13171/mjc8219040103fm.

17. Regti, A.; El Kassimi, A.; Laamari, M.R.; El Haddad, M. Competitive adsorption and optimization of binary mixture of textile dyes: A factorial design analysis. *Journal of the Association of Arab Universities for Basic and Applied Sciences* **2017**, *24*, 1-9, https://doi.org/10.1016/j.jaubas.2016.07.005.

18. Regti, A.; Laamari, M.R.; Stiriba, S.-E.; El Haddad, M. Use of response factorial design for process optimization of basic dye adsorption onto activated carbon derived from Persea species. *Microchem. J.* **2017**, *130*, 129-136, https://doi.org/10.1016/j.microc.2016.08.012.

19. Nadir, I.; Achour, Y.; El Kassimi, A.; El Himri, M.; Laamari, M.R.; El Haddad, M. Removal of Antibiotic Sulfamethazine from Aqueous Media. *Physical Chemistry Research* **2021**, *9*, 165-180, https://doi.org/10.22036/pcr.2020.249992.1839.

20. Garba, Z.; Rahim, A.; Hamza, S. Potential of Borassus aethiopum shells as precursor for activated carbon preparation by physico-chemical activation; Optimization, equilibrium and kinetic studies. *Journal of Environmental Chemical Engineering* **2014**, *2*, https://doi.org/10.1016/j.jece.2014.07.010.

21. Badri, N.; Chhiti, Y.; Bentiss, F.; Bensitel, M. Removal of cationic dye by high surface activated carbon prepared from biomass (date pits) by carbonization and activation processes. *Moroccan Journal of Chemistry* **2018**, *6*, 6-4.

22. Asfour, H.M.; Fadali, O.A.; Nassar, M.M.; El-Geundi, M.S. Equilibrium studies on adsorption of basic dyes on hardwood. *Journal of Chemical Technology and Biotechnology. Chemical Technology* **1985**, *35*, 21-27, https://doi.org/10.1002/jctb.5040350105.

23. Langmuir, I. The constitution and fundamental properties of solids and liquids. Part I. Solids. *J. Am. Chem. Soc.* **1916**, *38*, 2221-2295, https://doi.org/10.1021/ja02268a002.

24. Pourabadeh, A.; Baharinikoo, L.; Nouri, A.; Mehdizadeh, B.; Shojaei, S. The optimisation of operating parameters of dye removal: application of designs of experiments. *Int. J. Environ. Anal. Chem.* **2019**, 1-10, https://doi.org/10.1080/03067319.2019.1680657.

25. Parsaeian, M.R.; Dadfarnia, S.; Haji Shabani, A.M.; Hafezi Moghaddam, R. Green synthesis of a high capacity magnetic polymer nanocomposite sorbent based on the natural products for removal of Reactive Black 5. *Int. J. Environ. Anal. Chem.* **2020**, 1-15, https://doi.org/10.1080/03067319.2020.1748612.

26. Satapathy, M.K.; Das, P. Optimization of crystal violet dye removal using novel soil-silver nanocomposite as nanoadsorbent using response surface methodology. *Journal of Environmental Chemical Engineering* **2014**, *2*, 708-714, https://doi.org/10.1016/j.jece.2013.11.012.

27. Bagheri, A.R.; Ghaedi, M.; Hajati, S.; Ghaedi, A.M.; Goudarzi, A.; Asfaram, A. Random forest model for the ultrasonic-assisted removal of chrysoidine G by copper sulfide nanoparticles loaded on activated carbon; response surface methodology approach. *RSC Advances* **2015**, *5*, 59335-59343, https://doi.org/10.1039/C5RA08399K.

28. Mazaheri, H.; Ghaedi, M.; Asfaram, A.; Hajati, S. Performance of CuS nanoparticle loaded on activated carbon in the adsorption of methylene blue and bromophenol blue dyes in binary aqueous solutions: Using ultrasound power and optimization by central composite design. *J. Mol. Liq.* **2016**, *219*, 667-676, https://doi.org/10.1016/j.molliq.2016.03.050.

29. Ghaedi, M.; Rozkhoosh, Z.; Asfaram, A.; Mirtamizdoust, B.; Mahmoudi, Z.; Bazrafshan, A.A. Comparative studies on removal of Erythrosine using ZnS and AgOH nanoparticles loaded on activated carbon as adsorbents: Kinetic and isotherm studies of adsorption. *Spectrochimica Acta Part A: Molecular and Biomolecular Spectroscopy* **2015**, *138*, 176-186, https://doi.org/10.1016/j.saa.2014.10.046.

30. Tan, I.A.W.; Ahmad, A.L.; Hameed, B.H. Preparation of activated carbon from coconut husk: Optimization study on removal of 2,4,6-trichlorophenol using response surface methodology. *J. Hazard. Mater.* **2008**, *153*, 709-717, https://doi.org/10.1016/j.jhazmat.2007.09.014.

31. Oyekanmi, A.A.; Ahmad, A.; Hossain, K.; Rafatullah, M. Adsorption of Rhodamine B dye from aqueous solution onto acid treated banana peel: Response surface methodology, kinetics and isotherm studies. *PLoS One* **2019**, *14*, e0216878, https://doi.org/10.1371/journal.pone.0216878.

32. Liang, S.; Guo, X.; Tian, Q. Adsorption of Pb2+ and Zn2+ from aqueous solutions by sulfured orange peel. *Desalination* **2011**, *275*, 212-216, https://doi.org/10.1016/j.desal.2011.03.001.

33. Puziy, A.M.; Poddubnaya, O.I.; Martínez-Alonso, A.; Suárez-García, F.; Tascón, J.M.D. Surface chemistry of phosphorus-containing carbons of lignocellulosic origin. *Carbon* **2005**, *43*, 2857-2868, https://doi.org/10.1016/j.carbon.2005.06.014.

34. Karimi Darvanjooghi, M.H.; Davoodi, S.M.; Dursun, A.Y.; Ehsani, M.R.; Karimpour, I.; Ameri, E. Application of treated eggplant peel as a low-cost adsorbent for water treatment toward elimination of Pb^{2+}: Kinetic modeling and isotherm study. *Adsorption Science & Technology* **2018**, *36*, 1112-1143, https://doi.org/10.1177/0263617417753784.